

9148 8716  
NACA TN 2814

TECH LIBRARY KAFB, NM  
0065901

# NATIONAL ADVISORY COMMITTEE FOR AERONAUTICS

TECHNICAL NOTE 2814

THE APPLICATION OF PLANING CHARACTERISTICS TO THE  
CALCULATION OF THE WATER-LANDING LOADS AND  
MOTIONS OF SEAPLANES OF ARBITRARY  
CONSTANT CROSS SECTION

By Robert F. Smiley

Langley Aeronautical Laboratory  
Langley Field, Va.



Washington  
November 1952

AFMDC  
TECHNICAL LIBRARY  
AFL 2811



0065901

1U

## NATIONAL ADVISORY COMMITTEE FOR AERONAUTICS

## TECHNICAL NOTE 2814

THE APPLICATION OF PLANING CHARACTERISTICS TO THE  
CALCULATION OF THE WATER-LANDING LOADS AND  
MOTIONS OF SEAPLANES OF ARBITRARY  
CONSTANT CROSS SECTION

By Robert F. Smiley

## SUMMARY

The general equations governing the fixed-trim water landing of a straight-keel seaplane with a hull of arbitrary constant cross section are presented in such a form that the landing motions and loads are expressed in terms of the steady-planing characteristics of the seaplane. In order to verify the general validity of these equations, solutions are made for the water landing of a rectangular flat plate and are compared with experimental impact data. Calculated and experimental time histories of draft, velocity, and load are in good agreement. A survey is made of the available information on seaplane planing characteristics which is suitable for use with the analysis of the paper.

## INTRODUCTION

The National Advisory Committee for Aeronautics has undertaken an extensive program of theoretical and experimental research on hydrodynamic impact loads in order to establish a more rational foundation for water-loading requirements for the design of seaplanes. Most of the results of this program to date are contained in references 1 to 6. The development of the theory in these various papers usually proceeds substantially as follows: First, a theoretical or semiempirical analysis is made for the hydrodynamic forces acting during the two-dimensional impact of a body on a smooth water surface; the three-dimensional impact and planing case is then treated by assuming that the fluid flow occurs primarily in two-dimensional planes oriented normal to the keel and applying an approximate over-all correction to account for the difference between the two-dimensional and three-dimensional cases. This type of approach to the impact and planing problems has been found to provide fairly reasonable estimates of the impact loads on certain types of seaplane hulls (refs. 1 to 6), particularly those with scalloped bottoms and V-bottoms when the chines are not immersed below the water surface.

However, for impacts involving chine immersion, including impacts of a rectangular flat plate, accurate two-dimensional solutions have not yet been derived for all cases. For such cases, or for cases where greater accuracy is desired than can be obtained from the two-dimensional analogy, other procedures for computing impact loads and motions must be developed. The purpose of this paper is to develop such a procedure by relating the basic seaplane impact equations to the planing characteristics of a seaplane and to present the solution of these equations in such a form that the impact loads and motions may be calculated from these planing characteristics. This derivation begins with the same assumptions as were made in the preceding papers on impact theory (refs. 1 to 6), namely, that the instantaneous forces during a landing and in planing depend only on the components of motion normal to the keel. The differential equation of motion based on these assumptions is presented and then integrated to obtain equations for the time histories of the draft, velocity, and hydrodynamic load during an impact. The validity of the resulting equations is then tested by comparisons of experimental and calculated impact loads and motions for water landings of a rectangular flat plate. Finally, a survey and evaluation is made of the available information on the planing characteristics of seaplanes.

#### SYMBOLS

A	hydrodynamic aspect ratio, $\frac{(\text{Wetted length at keel})^2}{\text{Wetted area projected normal to keel}}$
b	beam of model, ft
$C_\beta$	function of angle of dead rise (0.750 for $\beta = 30^\circ$ )
$F_\zeta$	hydrodynamic force normal to keel (normal to surface for a flat plate), lb
$F_z$	vertical hydrodynamic force, lb
g	acceleration due to gravity, 32.2 ft/sec <sup>2</sup>
H	perpendicular distance between keel and plane of chines, ft
m	mass of model, slugs
$m_w$	virtual mass, slugs
$n_{1w}$	impact load factor, $F_z/mg$

R	wave-rise factor (see fig. 1(c))
t	time after water contact, sec
V	instantaneous resultant velocity of model, fps
$\dot{x}$	instantaneous velocity of model parallel to undisturbed water surface, fps
z	instantaneous draft of model normal to undisturbed water surface, ft
$\dot{z}$	instantaneous velocity of model normal to undisturbed water surface, fps
$\ddot{z}$	instantaneous acceleration of model normal to undisturbed water surface, ft/sec <sup>2</sup>
$\beta$	angle of dead rise, deg
$\gamma$	instantaneous flight-path angle relative to undisturbed water surface, $\tan^{-1} \frac{\dot{z}}{\dot{x}}$ , deg
$\zeta$	perpendicular distance between keel and point of initial water contact, ft
$\dot{\zeta}$	instantaneous velocity of model normal to keel (normal to model surface for a flat plate), $\dot{x} \sin \tau + \dot{z} \cos \tau$ , fps
$\ddot{\zeta}$	instantaneous acceleration of model normal to keel (normal to model surface for a flat plate), ft/sec <sup>2</sup>
$\lambda_{ch}$	wetted length at chines, beams
$\lambda_d$	length of model below undisturbed water surface, $\frac{z}{b \sin \tau}$ , beams
$\lambda_e$	wetted length at keel or longitudinal center line of model, beams
$\lambda_m$	mean wetted length, $\frac{\lambda_e + \lambda_{ch}}{2}$ , beams
$\dot{\xi}$	instantaneous velocity of model parallel to its longitudinal center line, $\dot{x} \cos \tau - \dot{z} \sin \tau$ , fps

$\rho$  mass density of water, 1.938 slugs/cu ft

$\tau$  trim, deg

$\phi(A)$  aspect-ratio correction

$\psi(\omega)$  psi-function,  $\frac{1}{\omega} + \log_e \omega - 1$

#### Subscripts:

ch at chine immersion

f rectangular flat plate

max maximum value

o at water contact

pl steady-planing conditions

r at rebound

#### Dimensionless variables:

$C_{\Delta}$  beam-loading coefficient,  $m/\rho b^3$

$C_B$  lift coefficient for steady planing,  $F_z/\frac{1}{2}\rho V_{pl}^2 b^2$

$$C_B' = \frac{C_B}{1 + \frac{m_w}{m}}$$

$C_L$  impact lift coefficient,  $F_z/\frac{1}{2}\rho V_o^2 b^2$

$C_V$  speed coefficient for steady planing (Froude number),  $V_{pl}/\sqrt{gb}$

$k$  generalized draft coefficient,  $\frac{1}{2C_{\Delta} \sin^2 \tau \cos^2 \tau} \int_0^{z/b} C_B' d\frac{z}{b}$

$\epsilon$  impact parameter,  $\tan(\gamma_o + \tau)/\tan \tau$

$\kappa$  impact approach parameter,  $\frac{\sin \tau}{\sin \gamma_o} \cos(\gamma_o + \tau)$

Dots are used to indicate derivatives with respect to time; for example,

$$\dot{z} = \frac{dz}{dt}; \quad \ddot{z} = \frac{d\dot{z}}{dt}$$

## ANALYSIS

### Derivation of Equation of Motion

In the first part of the analysis, the basic differential equation for the hydrodynamic loads and motions occurring during the oblique water impact of a straight-keel seaplane with a hull of arbitrary constant cross section is presented and then converted into such a form that the equation is expressed in terms of the conventional planing coefficient  $C_B$ . Throughout this analysis the seaplane is assumed to remain at a fixed trim and to have zero roll and yaw. The wing lift force acting on the seaplane is assumed to be equal to the weight of the seaplane, so that the net force acting to accelerate the seaplane is the hydrodynamic force.

During the landing of a long narrow body of constant cross section on a smooth water surface, the hydrodynamic force  $F_\xi$  on the body is generally assumed to be composed of two terms, one proportional to the square of the component of the model velocity normal to the keel  $\xi$  (see fig. 1) and one proportional to the normal deceleration of the body  $\ddot{\xi}$  (see, for example, ref. 1), or

$$F_\xi = D\dot{\xi}^2 + E\ddot{\xi} \quad (1)$$

where  $D$  and  $E$  are coefficients that depend on the instantaneous geometrical conditions (body shape, trim, and draft). The last term of equation (1) can be considered to represent the inertia force corresponding to the acceleration of the virtual mass of water associated with the impacting body; the coefficient  $E$  is thus equal to the virtual mass of water associated with the body ( $E = m_w$ ). A procedure for computing this quantity is given in appendix A. The coefficient  $D$  can be interpreted in terms of the conventional planing coefficient  $C_B$  as follows: In steady-planing tests the deceleration  $\ddot{\xi}$  is zero and the normal velocity is related to the planing velocity  $V_{pl}$  by the relation  $\dot{\xi} = V_{pl} \sin \tau$  (see fig. 1(a)). Also, the normal hydrodynamic force (neglecting friction) is related to the vertical force by the

relation  $F_z = F_\zeta \cos \tau$ . Substituting these relations into equation (1) gives for planing

$$F_z = DV_{pl}^2 \sin^2 \tau \cos \tau \quad (2)$$

Since the planing coefficient  $C_B$  is defined as

$$C_B = \frac{F_z}{\frac{1}{2} \rho V_{pl}^2 b^2} \quad (3)$$

a comparison of equations (2) and (3) shows that  $D$  is related to  $C_B$  by the equation

$$D = \frac{\rho b^2 C_B}{2 \sin^2 \tau \cos \tau} \quad (4)$$

By use of this relation (and  $E = m_w$ ), equation (1) can be rewritten as

$$F_\zeta = \frac{\rho b^2 C_B}{2 \sin^2 \tau \cos \tau} \dot{\zeta}^2 + m_w \ddot{\zeta} \quad (5)$$

Since the wing lift on the model has been assumed to be equal to the weight of the model, the hydrodynamic force is the net force acting on the model, and according to Newton's second law this force must be equal to the inertia reaction, or

$$F_\zeta = -m \ddot{\zeta} = \frac{\rho b^2 C_B}{2 \sin^2 \tau \cos \tau} \dot{\zeta}^2 + m_w \ddot{\zeta} \quad (6)$$

Equation (6) is the general differential equation for the force and motions for a seaplane landing, expressed in terms of the conventional planing coefficient  $C_B$ .

## Solution of Equation of Motion

In order to solve the differential equation of motion it is convenient first to rewrite equation (6) in the form

$$F_{\xi} = -m\ddot{\xi} = \frac{\rho b^2 C_B}{2 \sin^2 \tau \cos \tau \left(1 + \frac{m_w}{m}\right)} \dot{\xi}^2$$

Then, converting from normal force to vertical force by multiplying through by  $\cos \tau$  and abbreviating

$$C_B' = \frac{C_B}{1 + \frac{m_w}{m}} \quad (7)$$

gives the relation

$$F_Z = -m\ddot{\xi} \cos \tau = \frac{\rho b^2 C_B'}{2 \sin^2 \tau} \dot{\xi}^2 \quad (8)$$

The quantity  $C_B'$  for a given hull shape, weight, and trim depends on only one variable, the draft. On the other hand,  $\dot{\xi}$  and  $\ddot{\xi}$  depend on the two variables  $\xi$  and  $t$ ; equation (8) is thus an equation in three unknowns. In order to solve this equation one of these variables must be expressed in terms of the other two. The variable which is simplest to eliminate is  $\xi$ , which can be eliminated by the following substitutions (see fig. 1(b)):

$$\dot{\xi} = \frac{\dot{z}}{\cos \tau} + \dot{\xi} \tan \tau \quad (9)$$

$$\ddot{\xi} = \frac{\ddot{z}}{\cos \tau} \quad (10)$$

where  $\dot{\xi}$  is the component of the seaplane velocity parallel to the keel, which, from the previous assumptions of no friction drag and equal wing lift and float weight, is assumed to remain constant throughout any landing. Equation (8) can then be expressed in the form

$$-\frac{\ddot{z}}{\left(\frac{\dot{z}}{\cos \tau} + \dot{\xi} \tan \tau\right)^2} = \frac{\rho b^2 C_B'}{2m \sin^2 \tau}$$

or

$$-\frac{\ddot{z}}{(\dot{z} + \dot{\xi} \sin \tau)^2} dz = \frac{\rho b^2 C_B'}{2m \sin^2 \tau \cos^2 \tau} dz \quad (11)$$

Since  $\ddot{z} dz = \frac{dz}{dt} dz = \frac{dz}{dt} d\dot{z} = \dot{z} d\dot{z}$ , equation (11) can be also expressed in the form

$$-\frac{\dot{z} d\dot{z}}{(\dot{z} + \dot{\xi} \sin \tau)^2} = \frac{\rho b^2 C_B' dz}{2m \sin^2 \tau \cos^2 \tau}$$

or

$$-\frac{\frac{\dot{z}}{\dot{\xi} \sin \tau} d\frac{\dot{z}}{\dot{\xi} \sin \tau}}{\left(1 + \frac{\dot{z}}{\dot{\xi} \sin \tau}\right)^2} = \frac{\rho b^2 C_B' dz}{2m \sin^2 \tau \cos^2 \tau}$$

which can be easily integrated to give

$$\begin{aligned} \frac{\dot{\xi} \sin \tau}{\dot{z}_0 + \dot{\xi} \sin \tau} + \log_e \frac{\dot{z}_0 + \dot{\xi} \sin \tau}{\dot{\xi} \sin \tau} - \frac{\dot{\xi} \sin \tau}{\dot{z} + \dot{\xi} \sin \tau} - \log_e \frac{\dot{z} + \dot{\xi} \sin \tau}{\dot{\xi} \sin \tau} = \\ \frac{\rho b^2}{2m \sin^2 \tau \cos^2 \tau} \int_0^z C_B' dz \end{aligned} \quad (12)$$

The quantity on the right-hand side of equation (12), which depends only on the draft (for a given hull shape, weight, and trim), will henceforth be abbreviated as

$$k = \frac{\rho b^2}{2m \sin^2 \tau \cos^2 \tau} \int_0^z C_B' dz \quad (13)$$

and will be referred to as the generalized draft. An alternate form of equation (13), in terms of the beam-loading coefficient, is

$$k = \frac{1}{2C_{\Delta} \sin^2 \tau \cos^2 \tau} \int_0^{z/b} C_B' dz/b \quad (14)$$

where

$$C_{\Delta} = \frac{m}{\rho b^3} \quad (15)$$

In the remainder of this paper  $C_B$  is assumed to be a known function of draft which has been determined either experimentally or theoretically. Since all the other factors in equation (14) are known constants, except the quantity  $m_w/m$  which was used for converting  $C_B$  to  $C_B'$  and which can also be expressed as a function of draft as indicated in appendix A, the quantity  $k$  can also be considered as a known function of draft.

In order to compute the vertical hydrodynamic force from equation (8), equation (12) must be expressed in terms of  $\xi$  according to equation (9) as follows:

$$\left( \frac{1}{\frac{\dot{\xi}_0}{\dot{\xi} \tan \tau}} + \log_e \frac{\dot{\xi}_0}{\dot{\xi} \tan \tau} - 1 \right) - \left( \frac{1}{\frac{\dot{\xi}}{\dot{\xi} \tan \tau}} + \log_e \frac{\dot{\xi}}{\dot{\xi} \tan \tau} - 1 \right) = k \quad (16)$$

(The quantity 1 has been arbitrarily added and subtracted from the left-hand side of this equation for later convenience.) In order to facilitate computation, a function  $\psi$  is defined as follows:

$$\psi(\omega) = \frac{1}{\omega} + \log_e \omega - 1 \quad (17)$$

Equation (16) can be expressed in terms of the  $\psi$ -function as (compare eqs. (16) and (17))

$$\psi\left(\frac{\dot{\xi}_0}{\dot{\xi} \tan \tau}\right) - \psi\left(\frac{\dot{\xi}}{\dot{\xi} \tan \tau}\right) = k \quad (18a)$$

or

$$\psi\left(\frac{\dot{\xi}}{\dot{\xi} \tan \tau}\right) = \psi\left(\frac{\dot{\xi}_0}{\dot{\xi} \tan \tau}\right) - k \quad (18b)$$

or, in terms of the inverse function of  $\psi$ , as

$$\frac{\dot{\xi}}{\dot{\xi} \tan \tau} = \psi^{-1}\left[\psi\left(\frac{\dot{\xi}_0}{\dot{\xi} \tan \tau}\right) - k\right] \quad (18c)$$

or

$$\frac{\dot{\xi}}{\dot{\xi}_0} = \frac{\psi^{-1}\left[\psi\left(\frac{\dot{\xi}_0}{\dot{\xi} \tan \tau}\right) - k\right]}{\frac{\dot{\xi}_0}{\dot{\xi} \tan \tau}} \quad (18d)$$

The constant  $\dot{\xi}_0/\dot{\xi} \tan \tau$  will be henceforth abbreviated as  $\epsilon$ . Since  $\dot{\xi}$  (which equals  $\dot{\xi}_0$ ) is equal to  $\dot{\xi}_0 \cot(\gamma_0 + \tau)$  (see fig. 1(b)),  $\epsilon$  can also be expressed in the form

$$\epsilon = \frac{\dot{\xi}_0}{\dot{\xi} \tan \tau} = \frac{\tan(\gamma_0 + \tau)}{\tan \tau} \quad (19)$$

It is noted that this constant  $\epsilon$  is related to the impact approach parameter  $\kappa$  of reference 3 by the relation  $\epsilon = 1 + \frac{1}{\kappa}$ , where

$$\kappa = \frac{\sin \tau}{\sin \gamma_0} \cos(\gamma_0 + \tau)$$

The values of the  $\psi$ -function necessary for the use of equation (18d) are given in table I and in figures 2(a) and 2(b). The procedure for using figures 2(a) and 2(b) is illustrated in figure 2(c). For example, to compute the quantity  $\psi^{-1}[\psi(\epsilon) - k]$ , first find  $\epsilon$  on the  $\omega$ -axis. The corresponding ordinate is  $\psi(\epsilon)$ . Then go down on the  $\psi$ -axis a distance  $k$  to obtain  $\psi(\epsilon) - k$ . The quantity  $\psi^{-1}[\psi(\epsilon) - k]$  is then the

point on the  $\omega$ -axis corresponding to  $\psi(\epsilon) - k$  on the  $\psi$ -axis. (For more accurate results a similar procedure can be followed with the aid of table I.) It is noted that the inverse  $\psi$ -function is a double-valued function. The physical significance of this double-valued nature for the present problem is as follows: In each impact each value of draft (and of  $k$ ) is reached twice, once while the seaplane is going down into the water and once while it is coming out of the water. Values of  $\psi^{-1}[\psi(\epsilon) - k]$  greater than unity correspond to the descending motion and those less than unity correspond to the ascending motion.

The vertical hydrodynamic force is now obtained as a function of the generalized draft by combining equations (8), (18d), and (19) to yield

$$F_z = \frac{\rho b^2 \dot{\xi}^2 \tan^2 \tau}{2 \sin^2 \tau} C_B \left\{ \psi^{-1}[\psi(\epsilon) - k] \right\}^2$$

$$= \frac{\rho b^2 V_o^2 \cos^2(\gamma_o + \tau)}{2 \cos^2 \tau} C_B \left\{ \psi^{-1}[\psi(\epsilon) - k] \right\}^2 \quad (20)$$

The result may also be expressed as a dimensionless lift coefficient

$$C_L = \frac{F_z}{\frac{1}{2} \rho V_o^2 b^2} = \frac{\cos^2(\gamma_o + \tau)}{\cos^2 \tau} C_B \left\{ \psi^{-1}[\psi(\epsilon) - k] \right\}^2 \quad (21)$$

or as a load factor

$$n_{1w} = \frac{F_z}{mg} = \frac{\rho b^2 V_o^2 \cos^2(\gamma_o + \tau)}{2mg \cos^2 \tau} C_B \left\{ \psi^{-1}[\psi(\epsilon) - k] \right\}^2 \quad (22)$$

The vertical velocity can be related to the generalized draft by combining equations (9), (18c), and (19) to give

$$\frac{\dot{z}}{\dot{z}_o} = \frac{\psi^{-1}[\psi(\epsilon) - k] - 1}{\epsilon - 1} \quad (23)$$

The rebound (and initial) vertical velocity is obtained by setting the generalized draft equal to zero:

$$\frac{\dot{z}_r}{\dot{z}_0} = \frac{\psi^{-1}[\psi(\epsilon)] - 1}{\epsilon - 1} \quad (24)$$

It should be noted that the rebound velocity depends only on the impact parameter  $\epsilon$  and is not affected by the shape or mass of the seaplane.

The maximum draft is obtained by setting the vertical velocity equal to zero in equation (23) so that  $\psi^{-1}[\psi(\epsilon) - k_{\max}] = 1$  or  $\psi(\epsilon) - k_{\max} = \psi(1)$ , and since  $\psi(1) = 0$  (see table I),

$$k_{\max} = \psi(\epsilon) \quad (25)$$

where the relation between  $k_{\max}$  and  $z_{\max}$  is given by equation (14).

The relation between the time and the draft is given by

$$t = \int_0^t \frac{dt}{dz} dz = \int_0^z \frac{dz}{\dot{z}} \quad (26)$$

that is, a plot is made of the quantity  $1/\dot{z}$  against  $z$  and is graphically integrated to obtain the time.

A proposed procedure for computing impact loads and motions according to the preceding equations is given in appendix B.

### Substantiation of Theory

The results of the preceding derivation can be compared with experimental impact loads and motions in order to test the validity of these results and thus of the assumptions upon which the derivation is based. For the non-chine-immersed case the theory of the present paper is substantially the same as the theory of references 1 to 6; hence, the agreement between theory and experiment demonstrated in those papers for both the planing and the impact cases constitutes a verification of the theoretical equations of this paper. However, for impacts which involve more than a slight degree of chine immersion, such as those of a rectangular flat plate, no substantiation of the theory has been previously given.

To supply such a substantiation, experimental and calculated impact loads and motions for a rectangular flat plate are compared in figure 3. Experimental time histories of draft, vertical velocity, and hydrodynamic load are shown for five landings. The planing data needed for these calculations were obtained from reference 7 (see appendix C for details of computations) and the corresponding impact data were obtained from references 8 and 9. The good agreement shown in figure 3 for the calculated and experimental loads and motions substantiates the general validity of the impact equations. The small discrepancies that do exist are clearly within the limitations of accuracy of the experimental impact measurements.

### DISCUSSION OF PLANING DATA AND ANALYSES

In view of the preceding substantiation of the impact equations of this paper, the remaining problem is to provide reliable means of predicting the planing characteristics of seaplanes. The available information on this subject can, for convenience, be grouped into the following subdivisions: (1) the rectangular flat plate, (2) prismatic bodies with angles of dead rise greater than  $10^{\circ}$ , (3) prismatic bodies with angles of dead rise between  $0^{\circ}$  and  $10^{\circ}$ , and (4) prismatic bodies of arbitrary constant cross section. These various subdivisions will now be considered in detail.

#### The Rectangular Flat Plate

A large quantity of flat-plate planing data are available in references 7 and 10 to 13. However, much of this information is incomplete or was obtained at such low planing speeds that the buoyant forces (which are considered negligible during landings) are significant, and these data cannot always be safely extrapolated to find the high-speed (buoyancy-free) planing characteristics needed for impact calculations. Also, these available data are usually limited to relatively low trims or small ratios of wetted length to beam. Consequently, it is doubtful that the available data are adequate to cover all practical landing conditions.

The available analyses of flat-plate planing data, notably references 14 to 16, are all primarily empirical. They are consequently useful for interpolating the experimental data, but they cannot necessarily be extrapolated accurately beyond the range of the experimental data. One difficulty in using these empirical analyses is the fact that they are restricted to the determination of the relation between the planing coefficient  $C_B$  and the ratio of wetted length to beam, whereas for impact calculations the relation between  $C_B$  and the draft must be

known. In the case of the flat plate the water rises up in front of the plate (see fig. 1(d)) so that the wetted length  $\lambda_e$  materially exceeds the length of the model below the undisturbed water surface  $\lambda_d$ ,

where  $\lambda_d$  is related to the draft by the equation  $\lambda_d = \frac{z}{b \sin \tau}$ .

Planing data showing the relation between  $\lambda_e$  and  $\lambda_d$  are plotted in figure 4, together with a simple empirical equation fitting the data. This relation appears to be substantially independent of the trim for the range of data available, namely, for trims below  $18^\circ$ . For higher trims, according to impact data in reference 9, the wave rise  $\lambda_e - \lambda_d$  increases with increase of trim. (The quantity  $\lambda_e$  used in this paper roughly corresponds to the quantity  $\lambda_p$  in reference 9.)

#### Prismatic Bodies With Angles of Dead Rise Greater Than $10^\circ$

The problem of the determination of the planing characteristics of a V-bottom hull where the chines do not penetrate the water surface has been treated rather extensively, both theoretically and experimentally, in references 1, 3, 5, and 6 for angles of dead rise between  $10^\circ$  and  $40^\circ$ . However, when the chines do penetrate the water surface the analysis becomes more difficult. The first important problem is to determine when chine immersion occurs or, more specifically, the draft at which chine immersion occurs  $z_{ch}$ . Figure 1(c) shows that this occurs when the splashed-up water crosses the chines, or the draft is

$$z_{ch} = \frac{H \cos \tau}{R} = \frac{b \tan \beta \cos \tau}{2R} \quad (27)$$

(In fig. 1(c) water pile-up in front of the hull has been neglected, or  $\lambda_d = \lambda_e$ .) The wave-rise factor  $R$  has been evaluated in different ways by several investigators. According to Wagner's two-dimensional derivation for small angles of dead rise (ref. 17),  $R = \frac{\pi}{2}$ . This value of  $R$  is supported by the theoretical solutions of reference 18, which also show that  $R$  decreases with increase of dead-rise angle, and by the experimental data of reference 15 for angles of dead rise between  $10^\circ$  and  $30^\circ$ . Some full-scale landing data from a flying boat with  $20^\circ$  angle of dead rise (ref. 19) indicate a value of  $R = 1.4$ . The impact theory of reference 3 uses a value of  $R = \left(\frac{\pi}{2\beta} - .1\right) \tan \beta$  and reference 6 uses a value of  $R = 1$ . It should be noted that the last two values of  $R$  do not directly correspond to the physical water splash-up but are, rather,

effective values of splash-up. The first value of  $R$  was proposed from considerations of the over-all load problem and the second value resulted from the semiempirical analysis of planing data given in reference 6. In view of these observations it appears that  $R$  is approximately equal to  $\pi/2$ ; however, further research on this subject would be of value.

Various analyses have been made for the planing coefficients of the V-bottom hull with chines substantially immersed, notably those of references 6, 15, and 20. Reference 6 presents a semiempirical treatment of the problem which also considers the effects of buoyancy on the planing loads. In order to bring this treatment into agreement with the extremely limited data available at that time (refs. 6, 11, and 13) it was necessary to assume that the wave-rise factor  $R$  was equal to 1. Recently, more V-bottom planing data have been published (ref. 15), and from a consideration of these data as well as from the consideration of some impact data (to be discussed subsequently) for a float with  $30^\circ$  angle of dead rise, the analysis of reference 6 still appears reasonable for its two end-point conditions, the non-chine-immersed case and the deeply chine-immersed case, but it is somewhat conservative in the intermediate range as a result of the assumption that the wave-rise factor is unity. In reference 15, where the more recent data are used, an empirical analysis restricted to the case of the chine-immersed hull is given which corresponds to the more realistic splash-up factor of  $\pi/2$  and which is in fair agreement with the available experimental data. (A somewhat parallel but less detailed treatment is given in reference 20.) However, since the available data are still not very extensive and do not adequately cover the practical limits of large ratios of wetted length to beam, it is not yet certain that the empirical formula of reference 15 can be safely extrapolated to large ratios of wetted length to beam. Therefore, a need apparently exists for further study of the planing characteristics of V-bottom hulls with angles of dead rise greater than  $10^\circ$  for the case of considerable chine immersion.

As a test of the relative merits of the two planing equations of references 6 and 15, calculations based on these two formulas were made for the landing loads on a prismatic V-bottom hull having an angle of dead rise of  $30^\circ$  and are compared with experimental impact data in figure 5. (Since the analysis of reference 15 is restricted to the chine-immersed case, the planing coefficients prior to chine immersion were in both cases determined from the equation of reference 6 as is discussed in appendix D.) At the low flight-path angle ( $\gamma_0 = 2.2^\circ$ ) of figure 5(a), which corresponds to a landing in which the chines become immersed, but not deeply, the analysis of reference 15 gives much better agreement with the experimental impact data both in the shape of the load time history and in the magnitudes. This better agreement is due to the fact that reference 15 makes use of a more realistic estimate of the draft at which chine immersion begins than does reference 6. From an examination of figure 5(b), which gives computed and experimental data for a large flight-path angle ( $\gamma_0 = 5.9^\circ$ ) which corresponds to substantial chine immersion,

both analyses give reasonable qualitative representations of the load time history, reference 6 being somewhat conservative and reference 15 being somewhat unconservative. Additional calculated and experimental impact load data shown in figure 5(c) substantiate these observations. In figure 5(d) are shown calculated and experimental maximum drafts. These indicate the same conclusions as the load comparison; the maximum draft is underestimated by reference 6 (which is the same as overestimating the load) and reference 15 tends to overestimate the draft.

To summarize the preceding discussion of the planing coefficients for angles of dead rise greater than  $10^\circ$ , the use of the equations of references 6 and 15 apparently results in a reasonable calculation of the landing loads, reference 6 giving somewhat conservative results and reference 15 giving somewhat unconservative results. However, for greater accuracy further planing research seems to be needed.

#### Prismatic Bodies With Angles of Dead Rise Between $0^\circ$ and $10^\circ$

As yet no experimental data are available to test the existing analyses for angles of dead rise between  $0^\circ$  and  $10^\circ$ . The analysis of reference 6 is known to be inadequate for the case of  $0^\circ$  angle of dead rise; therefore, it is as yet somewhat doubtful that this equation can be used in this range ( $0^\circ < \beta < 10^\circ$ ). The equation of reference 15, by the nature of its derivation, can be reasonably assumed to apply for dead-rise angles in this range. However, one difficulty arises in the use of this equation in this range. The results of reference 15 are essentially expressed in such a form that the planing coefficient is related to the wetted length at the keel ( $\lambda_e$  in fig. 1(d)) rather than to the draft. For angles of dead rise greater than  $10^\circ$ , reference 15 states that the relation between the draft and the wetted length at the keel is approximately equal to the sine of the trim ( $\lambda_e = \lambda_d = \frac{Y}{b \sin \tau}$ ). However, for the case of the flat plate ( $0^\circ$  angle of dead rise) this relation was previously shown to be considerably more complicated because of the wave rise in front of the plate (see fig. 1(d)). Thus, if reliable computations are to be made for the landing loads for V-bottom surfaces with angles of dead rise between  $0^\circ$  and  $10^\circ$ , a need exists for an investigation of the wave-rise effects in this range.

#### Prismatic Bodies of Arbitrary Constant Cross Section

For prismatic hulls of arbitrary constant cross section, little experimental information is available on planing characteristics (ref. 11). However, reference 2 presents a theoretical means of analysis which is applicable to hulls of constant cross section without reflex chines or chine strips, and which has been partly substantiated by some experimental impact data in the same reference.

## CONCLUDING REMARKS

The equations for the landing impact of a seaplane with a hull of arbitrary constant cross section have been presented in such a form that the landing loads and motions are expressed in terms of the planing properties of the seaplane. Comparisons of calculated and experimental loads and motions for the landing of a rectangular flat plate have shown that this analysis is valid for a greater range of conditions than was covered by previous papers. A survey and evaluation of the available information on seaplane planing characteristics which is suitable for use with the analysis of this paper has indicated a need for further research on these characteristics.

Langley Aeronautical Laboratory  
National Advisory Committee for Aeronautics  
Langley Field, Va., July 7, 1952

## APPENDIX A

## VIRTUAL MASS

In reference 2 an approximate expression is given for the virtual mass of a body of arbitrary constant cross section prior to chine immersion. This equation, converted to the terminology of the present paper, is

$$\frac{m_w}{m} = \frac{1}{2C_\Delta \sin^2 \tau \cos^2 \tau} \int_0^{z/b} C_B \frac{dz}{b} \quad (A1)$$

This relation, substituted into equation (14), gives

$$\begin{aligned} k &= \int_0^{z/b} \frac{\frac{1}{2C_\Delta \sin^2 \tau \cos^2 \tau} C_B \frac{dz}{b}}{1 + \frac{1}{2C_\Delta \sin^2 \tau \cos^2 \tau} \int_0^{z/b} C_B \frac{dz}{b}} \\ &= \log_e \left( 1 + \frac{1}{2C_\Delta \sin^2 \tau \cos^2 \tau} \int_0^{z/b} C_B \frac{dz}{b} \right) \end{aligned} \quad (A2)$$

prior to chine immersion.

Subsequent to chine immersion the virtual mass  $m_{wch}$  associated with the wetted area forward of the intersection of the chines and the water surface can be computed from equation (A1). The virtual mass of the region aft of this intersection can be approximated by a semicylinder of water circumscribed about the beam and corrected for the finite aspect ratio. The resulting equation for the virtual mass is

$$m_w = m_{wch} + \frac{\rho \pi b^3}{8} \lambda_{ch} \phi(A) \quad ; \quad (z \geq z_{ch}) \quad (A3)$$

or

$$\frac{m_w}{m} = \frac{m_{wch}}{m} + \frac{\rho \pi b^3}{8m} \lambda_{ch} \varphi(A) = \frac{1}{2C_{\Delta} \sin^2 \tau \cos^2 \tau} \int_0^{z_{ch}/b} C_B \frac{dz}{b} + \frac{\pi}{8C_{\Delta}} \lambda_{ch} \varphi(A) \quad (z \geq z_{ch}) \quad (A4)$$

where  $\varphi(A)$  is the aspect-ratio correction. For cases where the water does not splash up in front of the model, the wetted chine length  $\lambda_{ch}$

(see fig. 1(d)) is equal to  $\frac{z - z_{ch}}{b \sin \tau}$  and equation (A4) becomes

$$\frac{m_w}{m} = \frac{1}{2C_{\Delta} \sin^2 \tau \cos^2 \tau} \int_0^{z_{ch}/b} C_B \frac{dz}{b} + \frac{\pi \varphi(A)}{8C_{\Delta} \sin \tau} \left( \frac{z}{b} - \frac{z_{ch}}{b} \right) \quad (z \geq z_{ch}) \quad (A5)$$

For the flat plate the wetted chine length is the total wetted length ( $\lambda_{ch} = \lambda_e$ ) and equation (A4) becomes

$$\frac{m_w}{m} = \frac{\pi}{8C_{\Delta}} \lambda_e \varphi(A) \quad (A6)$$

For arbitrary shapes with splash-up in front, the use of equation (A5) is suggested. The error introduced by neglecting the splash-up for this purpose will usually be small or negligible.

According to Pabst (refs. 21 and 22) the virtual mass of a rectangular flat plate of aspect ratio  $A$ , as determined by vibration tests, is equal to that of a circumscribed cylinder times the quantity  $\varphi(A)$ , where

$$\varphi(A) = \sqrt{\frac{1}{1 + \frac{1}{A^2}}} \left( 1 - \frac{0.425}{A + \frac{1}{A}} \right) \quad (0 < A < \infty) \quad (A7)$$

which can be approximated as

$$\varphi(A) = 1 - \frac{1}{2A} \quad (A > 1.5)$$

These relations are suggested for use in the computations of the aspect-ratio correction for models of arbitrary shape, provided that the aspect ratio of the model can be computed as a function of draft without too much difficulty. If this procedure is difficult, however, the aspect-ratio correction may be considered approximately equal to unity:

$$\phi(A) \approx 1 \quad (A9)$$

For cases where  $A$  is reasonably large, no significant error should result from the substitution of equation (A9) into equation (A5).

The hydrodynamic aspect ratio of a model is, by definition, equal to the quotient of the square of the keel wetted length and the projected wetted area normal to the keel. Thus, for a rectangular flat plate,

$$A = \lambda_e \quad (A10)$$

and, for a wedge of dead-rise angle  $\beta$  with no forward splash-up of water,

$$A = \frac{\left(\frac{z}{b}\right)^2 \csc \tau}{\frac{z}{b} - \frac{\tan \beta \cos \tau}{4R}} \quad (A11)$$

## APPENDIX B

## PROPOSED PROCEDURE FOR COMPUTATIONS OF IMPACT LOADS AND MOTIONS

In order to utilize the equations of this paper to compute the water loads and motions of a seaplane, the following procedure is suggested:

- (1) Select values of  $C_{\Delta}$ ,  $\tau$ ,  $\gamma_0$ , and  $V_0$ .
- (2) Make a plot of  $C_B$  against  $z/b$ . This plot may be obtained from experimental planing data or by utilizing theoretical planing equations.
- (3) Graphically or analytically integrate the  $C_B$  curve to obtain the quantity  $\int_0^{z/b} C_B \frac{dz}{b}$  as a function of draft.
- (4) Compute  $m_w/m$  as a function of draft according to equations (A1) and (A5). (For slightly better accuracy in the case of the rectangular flat plate, use equation (A6), together with the empirical curve in figure 4, instead.)
- (5) Compute  $C_B'$  as a function of draft according to equation (7).
- (6) Compute  $k$  as a function of draft according to equation (14).
- (7) Compute  $\epsilon$  from equation (19) and then  $\psi(\epsilon)$  from table I or figure 2.
- (8) Select a series of values of  $k$  between 0 and  $\psi(\epsilon)$ .
- (9) For each value of  $k$  (the generalized draft), compute  $\psi^{-1}[\psi(\epsilon) - k]$  as indicated in figure 2(c), with the aid of table I or figure 2(a) or 2(b). (The larger value of  $\psi^{-1}[\psi(\epsilon) - k]$  obtained corresponds to the seaplane descending into the water and the smaller value corresponds to the seaplane rising out of the water.)
- (10) Compute the vertical force from equation (20), (21), or (22). Plot this quantity against draft. The maximum load can then be obtained from this curve.

(11) Obtain the vertical velocity as a function of draft from equation (23).

(12) Obtain the relation between draft and time by graphical integration of equation (26).

## APPENDIX C

## DETAILS OF COMPUTATIONS FOR FLAT PLATE

The impact loads and motions shown in figure 3 for the rectangular flat plate were computed according to the procedure of appendix B. The relations between  $C_B$  and  $z/b$  needed for step (2) of that procedure were obtained as follows. The relation between the wetted length  $\lambda_e$  and the planing coefficient  $C_B$  was obtained from a cross plot of Locke's high-speed planing data from reference 7 (see fig. 6). The relation between the draft and the wetted length was obtained from figure 4, which is a plot of data obtained by Sottorf (ref. 10) and Sambraus (ref. 12). The empirical formula shown in this figure was used for all computations. The relation between  $C_B$  and  $z/b$  was obtained by combining figure 6 with the empirical formula from figure 4.

## APPENDIX D

DETAILS OF COMPUTATIONS FOR  $30^\circ$  ANGLE OF DEAD RISE

The impact loads and motions shown in figure 5 for a model with  $30^\circ$  angle of dead rise were computed according to the procedure of appendix B. The relation between  $C_B$  and  $z/b$  needed for step (2) of that procedure was obtained from the following equations taken from references 6 and 15:

According to reference 6 (if buoyancy be neglected),

$$\left. \begin{aligned} C_B &= 1.42\pi \cot^2 \beta \sin \tau \left(1 - \frac{\tan \tau}{2 \tan \beta}\right) \left(\frac{z}{b}\right)^2 & (z < z_{ch}) \\ C_B &= 0.355\pi \sin \tau \cos^2 \tau \left[1 - \frac{\sin \tau \left(\frac{z}{b} - \frac{\tan \beta}{4}\right)}{2 \left(\frac{z}{b}\right)^2}\right] + \\ &\quad C_s \sin \tau \cos \tau \left(\frac{z}{b} - \frac{\tan \beta \cos \tau}{2}\right) & (z > z_{ch}) \\ R &= 1 \end{aligned} \right\} \quad (D1)$$

where  $C_s$  is a function of dead-rise angle tabulated in reference 6 (0.750 for  $\beta = 30^\circ$ ).

According to reference 15, for the chine-immersed case only (if buoyancy be neglected),

$$\left. \begin{aligned} C_B &= C_{B_f} - 0.0065\beta C_{B_f}^{0.6} \\ R &= \frac{\pi}{2} \end{aligned} \right\} \quad (z > z_{ch}) \quad (D2)$$

where

$$C_{B_F} = 0.0120 \lambda_m^{1/2} \tau^{1.1}$$

$$\lambda_m = \frac{1}{2}(\lambda_e + \lambda_{ch})$$

$$\lambda_e = \frac{z}{b \sin \tau}$$

$$\lambda_{ch} = \lambda_e - \frac{\tan \beta}{\pi \tan \tau}$$

Since equation (D2) is not valid for the case of no chine immersion, in order to use this equation for impact computations equation (D1) was used to predict the planing coefficient prior to chine immersion. Chine immersion was taken to occur at the draft at which equations (D1) and (D2) predicted the same planing coefficient. This procedure for determining chine immersion was chosen only because for the specific case considered ( $\beta = 30^\circ$ ,  $\tau = 15^\circ$ ) this value of draft corresponded to a wave-rise factor of roughly  $\pi/2$ , which is in agreement with the value predicted by equation (D2).

## REFERENCES

1. Mayo, Wilbur L.: Analysis and Modification of Theory for Impact of Seaplanes on Water. NACA Rep. 810, 1945. (Supersedes NACA TN 1008.)
2. Milwitzky, Benjamin: A Theoretical Investigation of Hydrodynamic Impact Loads on Scalloped-Bottom Seaplanes and Comparisons With Experiment. NACA Rep. 867, 1947. (Supersedes NACA TN 1363.)
3. Milwitzky, Benjamin: A Generalized Theoretical and Experimental Investigation of the Motions and Hydrodynamic Loads Experienced by V-Bottom Seaplanes During Step-Landing Impacts. NACA TN 1516, 1948.
4. Milwitzky, Benjamin: A Generalized Theoretical Investigation of the Hydrodynamic Pitching Moments Experienced by V-Bottom Seaplanes During Step-Landing Impacts and Comparisons With Experiment. NACA TN 1630, 1948.
5. Benscoter, Stanley U.: Impact Theory for Seaplane Landings. NACA TN 1437, 1947.
6. Steiner, Margaret F.: Analysis of Planing Data for Use in Predicting Hydrodynamic Impact Loads. NACA TN 1694, 1948.
7. Locke, F. W. S., Jr.: Tests of a Flat Bottom Planing Surface To Determine the Inception of Planing. NAVAER DR Rep. 1096, Bur. Aero., Dec. 1948.
8. McArver, A. Ethelda: Water-Landing Investigation of a Model Having Heavy Beam Loadings and  $0^\circ$  Angle of Dead Rise. NACA TN 2330, 1951.
9. Smiley, Robert F.: An Experimental Study of Water-Pressure Distributions During Landings and Planing of a Heavily Loaded Rectangular Flat-Plate Model. NACA TN 2453, 1951.
10. Sottorf, W.: Experiments With Planing Surfaces. NACA TM 661, 1932.
11. Sottorf, W.: Experiments With Planing Surfaces. NACA TM 739, 1934.
12. Sambraus, A.: Planing-Surface Tests at Large Froude Numbers - Airfoil Comparison. NACA TM 848, 1938.
13. Shoemaker, James M.: Tank Tests of Flat and V-Bottom Planing Surfaces. NACA TN 509, 1934.

14. Locke, F. W. S., Jr.: An Empirical Study of Low Aspect Ratio Lifting Surfaces With Particular Regard to Planing Craft. Jour. Aero. Sci., vol. 16, no. 3, Mar. 1949, pp. 184-188.
15. Korvin-Kroukovsky, B. V., Savitsky, Daniel, and Lehman, William F.: Wetted Area and Center of Pressure of Planing Surfaces. Preprint No. 244, S.M.F. Fund Paper, Inst. Aero. Sci. (Rep. No. 360, Project No. NRO62-012, Office Naval Res., Exp. Towing Tank, Stevens Inst. Tech., Aug. 1949.)
16. Sedov, L.: Scale Effect and Optimum Relations for Sea Surface Planing. NACA TM 1097, 1947.
17. Wagner, Herbert: Über Stoss- und Gleitvorgänge an der Oberfläche von Flüssigkeiten. Z.f.a.M.M., Bd. 12, Heft 4, Aug. 1932, pp. 193-215.
18. Pierson, John D.: The Penetration of a Fluid Surface by a Wedge. S.M.F. Fund Paper No. FF-3, Inst. Aero. Sci. (Rep. No. 381, Project No. NRO62-012, Office Naval Res., Exp. Towing Tank, Stevens Inst. Tech.), July 1950.
19. Steiner, Margaret F.: Comparison of Over-All Impact Loads Obtained During Seaplane Landing Tests With Loads Predicted by Hydrodynamic Theory. NACA TN 1781, 1949.
20. Locke, F. W. S., Jr.: Planing Efficiency As Affected by Deadrise. NAVAER DR Rep. 1132, Bur. Aero., July 1949.
21. Pabst, Wilhelm: Theory of the Landing Impact of Seaplanes. NACA TM 580, 1930.
22. Pabst, Wilhelm: Landing Impact of Seaplanes. NACA TM 624, 1931.
23. Batterson, Sidney A., and McArver, A. Ethelda: Water Landing Investigation of a Model Having a Heavy Beam Loading and a 30° Angle of Dead Rise. NACA TN 2015, 1950.

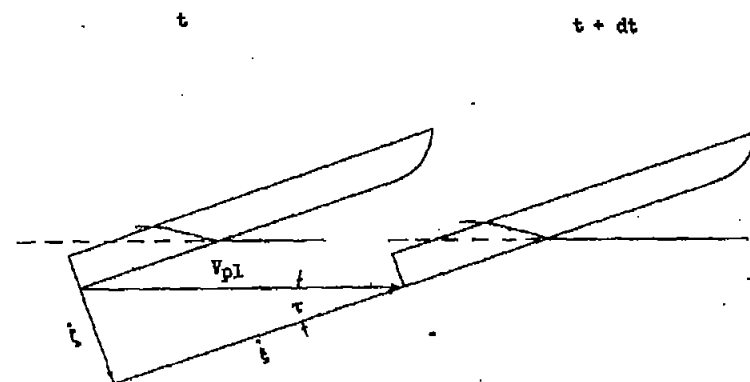
TABLE I. -  $\Psi$ -FUNCTION

$$\Psi(m) = \frac{1}{m} + \log_e m - 1$$

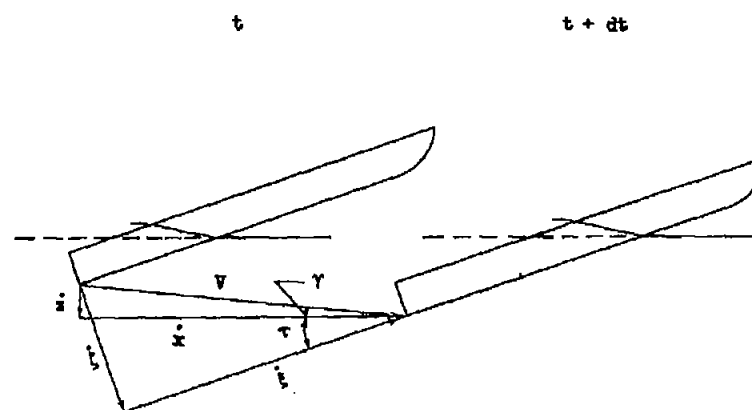
m	$\Psi(m)$	m	$\Psi(m)$	m	$\Psi(m)$	m	$\Psi(m)$	m	$\Psi(m)$	m	$\Psi(m)$	m	$\Psi(m)$	m	$\Psi(m)$
0.01	94.3948	0.41	0.5474	0.81	0.0239	1.21	0.0171	1.61	0.0973	2.01	0.1956	2.41	0.2946	2.81	0.3891
.02	45.0880	.42	.5135	.82	.0210	1.22	.0185	1.62	.0997	2.02	.1982	2.42	.2970	2.82	.3914
.03	28.8267	.43	.4816	.83	.0185	1.23	.0200	1.63	.1021	2.03	.2007	2.43	.2994	2.83	.3936
.04	20.7811	.44	.4517	.84	.0161	1.24	.0216	1.64	.1045	2.04	.2032	2.44	.3018	2.84	.3959
.05	16.0043	.45	.4237	.85	.0140	1.25	.0231	1.65	.1068	2.05	.2056	2.45	.3043	2.85	.3982
.06	12.8533	.46	.3974	.86	.0120	1.26	.0248	1.66	.1092	2.06	.2082	2.46	.3067	2.86	.4005
.07	10.6264	.47	.3727	.87	.0101	1.27	.0264	1.67	.1116	2.07	.2106	2.47	.3091	2.87	.4027
.08	8.9742	.48	.3493	.88	.0086	1.28	.0281	1.68	.1140	2.08	.2131	2.48	.3115	2.88	.4050
.09	7.7032	.49	.3275	.89	.0071	1.29	.0298	1.69	.1165	2.09	.2156	2.49	.3139	2.89	.4073
.10	6.6974	.50	.3068	.90	.0057	1.30	.0316	1.70	.1189	2.10	.2181	2.50	.3163	2.90	.4095
.11	5.8836	.51	.2875	.91	.0046	1.31	.0334	1.71	.1213	2.11	.2206	2.51	.3187	2.91	.4118
.12	5.2130	.52	.2692	.92	.0036	1.32	.0352	1.72	.1237	2.12	.2231	2.52	.3211	2.92	.4141
.13	4.6521	.53	.2519	.93	.0027	1.33	.0371	1.73	.1262	2.13	.2256	2.53	.3235	2.93	.4163
.14	4.1768	.54	.2357	.94	.0019	1.34	.0389	1.74	.1286	2.14	.2281	2.54	.3259	2.94	.4186
.15	3.7696	.55	.2204	.95	.0013	1.35	.0408	1.75	.1311	2.15	.2306	2.55	.3283	2.95	.4208
.16	3.4174	.56	.2059	.96	.0009	1.36	.0428	1.76	.1335	2.16	.2331	2.56	.3306	2.96	.4230
.17	3.1104	.57	.1923	.97	.0004	1.37	.0447	1.77	.1360	2.17	.2356	2.57	.3330	2.97	.4253
.18	2.8408	.58	.1794	.98	.0002	1.38	.0467	1.78	.1384	2.18	.2380	2.58	.3354	2.98	.4275
.19	2.6025	.59	.1673	.99	.0000	1.39	.0487	1.79	.1409	2.19	.2405	2.59	.3378	2.99	.4297
.20	2.3906	.60	.1559	1.00	.0000	1.40	.0508	1.80	.1434	2.20	.2430	2.60	.3401	3.00	.4319
.21	2.2013	.61	.1450	1.01	.0001	1.41	.0528	1.81	.1458	2.21	.2455	2.61	.3425	3.10	.4340
.22	2.0314	.62	.1349	1.02	.0002	1.42	.0549	1.82	.1483	2.22	.2480	2.62	.3449	3.20	.4377
.23	1.8781	.63	.1253	1.03	.0004	1.43	.0570	1.83	.1508	2.23	.2504	2.63	.3472	3.30	.4407
.24	1.7296	.64	.1162	1.04	.0007	1.44	.0591	1.84	.1534	2.24	.2529	2.64	.3496	3.40	.4439
.25	1.5937	.65	.1077	1.05	.0012	1.45	.0612	1.85	.1557	2.25	.2554	2.65	.3519	3.50	.4471
.26	1.4699	.66	.0997	1.06	.0017	1.46	.0634	1.86	.1582	2.26	.2578	2.66	.3543	3.60	.4503
.27	1.3544	.67	.0920	1.07	.0022	1.47	.0655	1.87	.1607	2.27	.2603	2.67	.3566	3.70	.4535
.28	1.2484	.68	.0849	1.08	.0029	1.48	.0677	1.88	.1632	2.28	.2628	2.68	.3590	3.80	.4567
.29	1.1510	.69	.0782	1.09	.0036	1.49	.0699	1.89	.1657	2.29	.2652	2.69	.3613	3.90	.4599
.30	1.0623	.70	.0719	1.10	.0044	1.50	.0721	1.90	.1682	2.30	.2677	2.70	.3636	4.00	.4631
.31	0.9816	.71	.0660	1.11	.0053	1.51	.0744	1.91	.1707	2.31	.2702	2.71	.3660	4.10	.4663
.32	.9086	.72	.0604	1.12	.0062	1.52	.0766	1.92	.1732	2.32	.2726	2.72	.3683	4.20	.4695
.33	.8426	.73	.0552	1.13	.0072	1.53	.0789	1.93	.1757	2.33	.2751	2.73	.3706	4.30	.4727
.34	.7824	.74	.0503	1.14	.0082	1.54	.0811	1.94	.1782	2.34	.2775	2.74	.3729	4.40	.4759
.35	.7273	.75	.0456	1.15	.0093	1.55	.0834	1.95	.1807	2.35	.2800	2.75	.3752	4.50	.4791
.36	.6762	.76	.0414	1.16	.0105	1.56	.0857	1.96	.1831	2.36	.2824	2.76	.3776	4.60	.4823
.37	.6284	.77	.0373	1.17	.0117	1.57	.0880	1.97	.1856	2.37	.2848	2.77	.3799	4.70	.4855
.38	.5840	.78	.0336	1.18	.0130	1.58	.0903	1.98	.1882	2.38	.2873	2.78	.3822	4.80	.4887
.39	.5425	.79	.0301	1.19	.0143	1.59	.0927	1.99	.1906	2.39	.2897	2.79	.3845	4.90	.4919
.40	.5037	.80	.0269	1.20	.0156	1.60	.0950	2.00	.1932	2.40	.2921	2.80	.3868	5.00	.4951

<sup>a</sup>For values of  $m$  greater than 3, the values of the  $\Psi$ -function were computed from table I of reference 5.

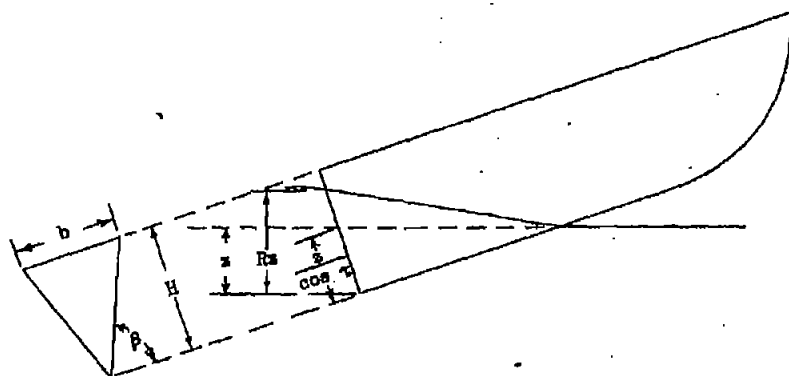
NACA



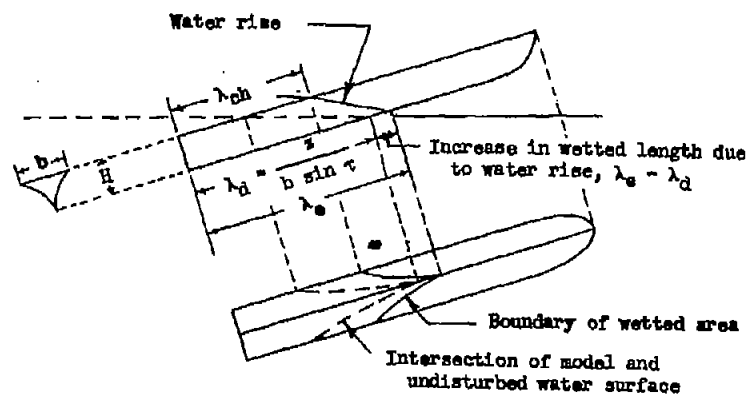
(a) Velocity relations in planing.



(b) Velocity relations in impacts.



(c) Non-chine-immersed prismatic float.



(d) Chine-immersed float of arbitrary constant cross section.



Figure 1.- Geometrical relations.

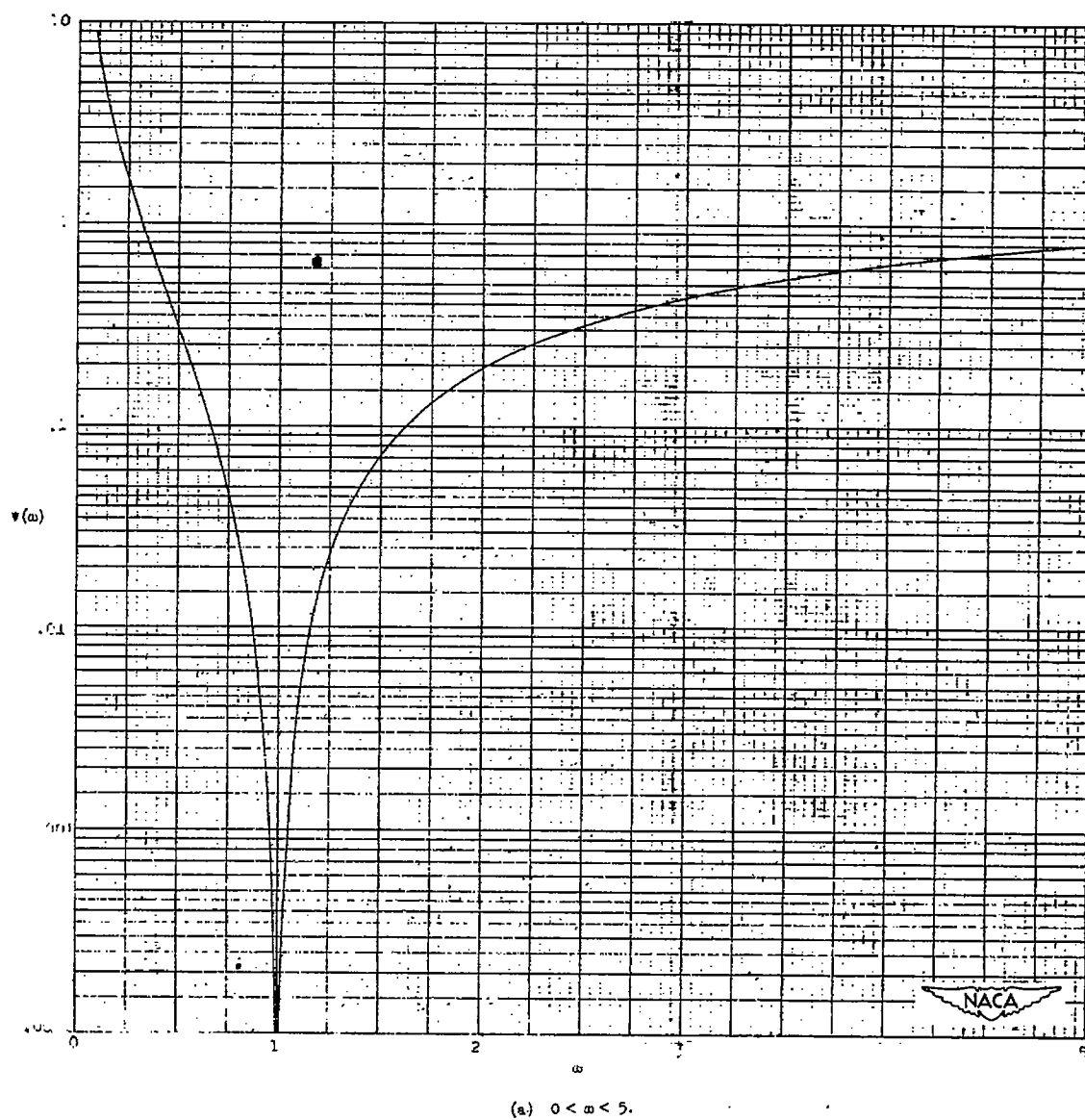
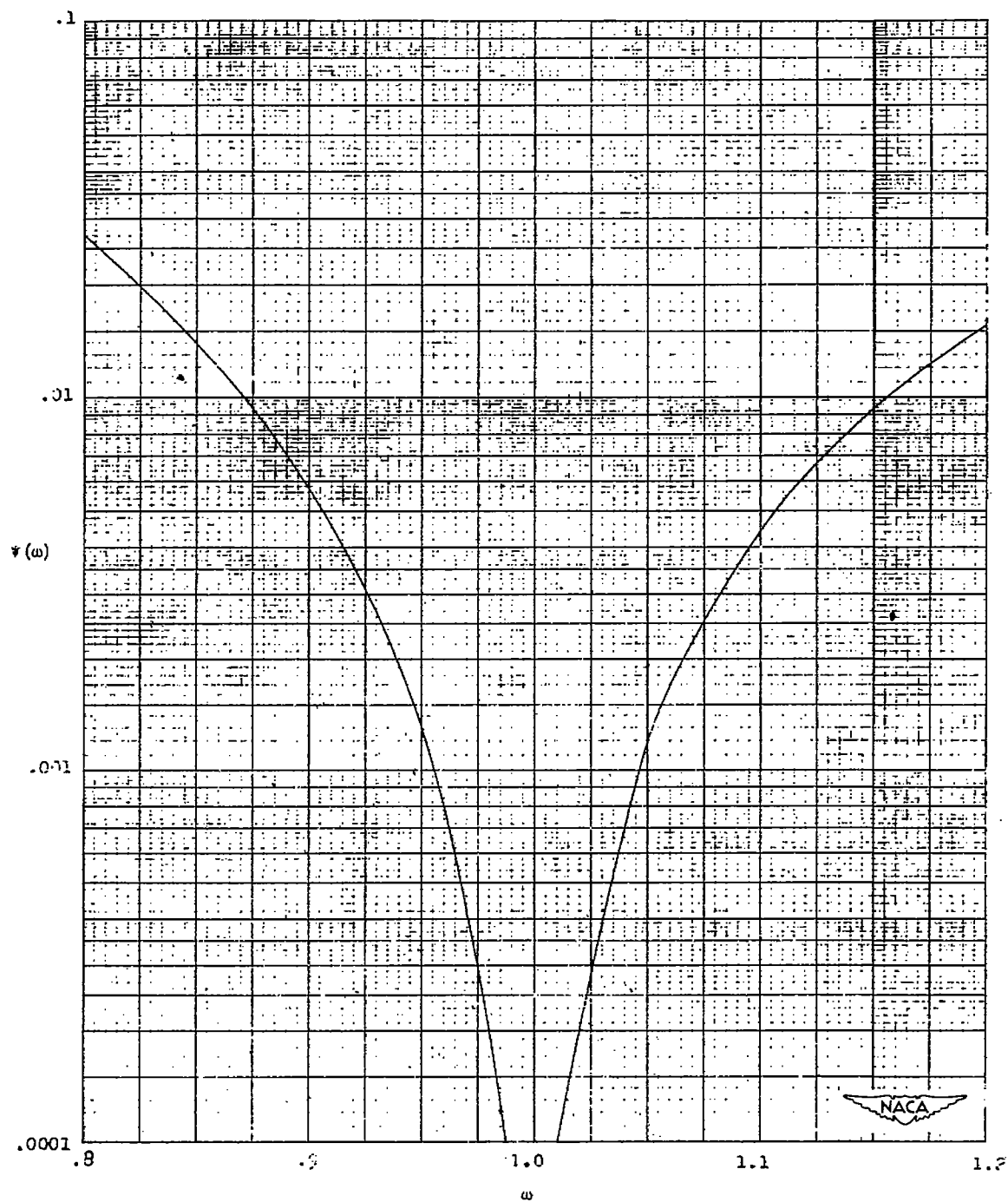
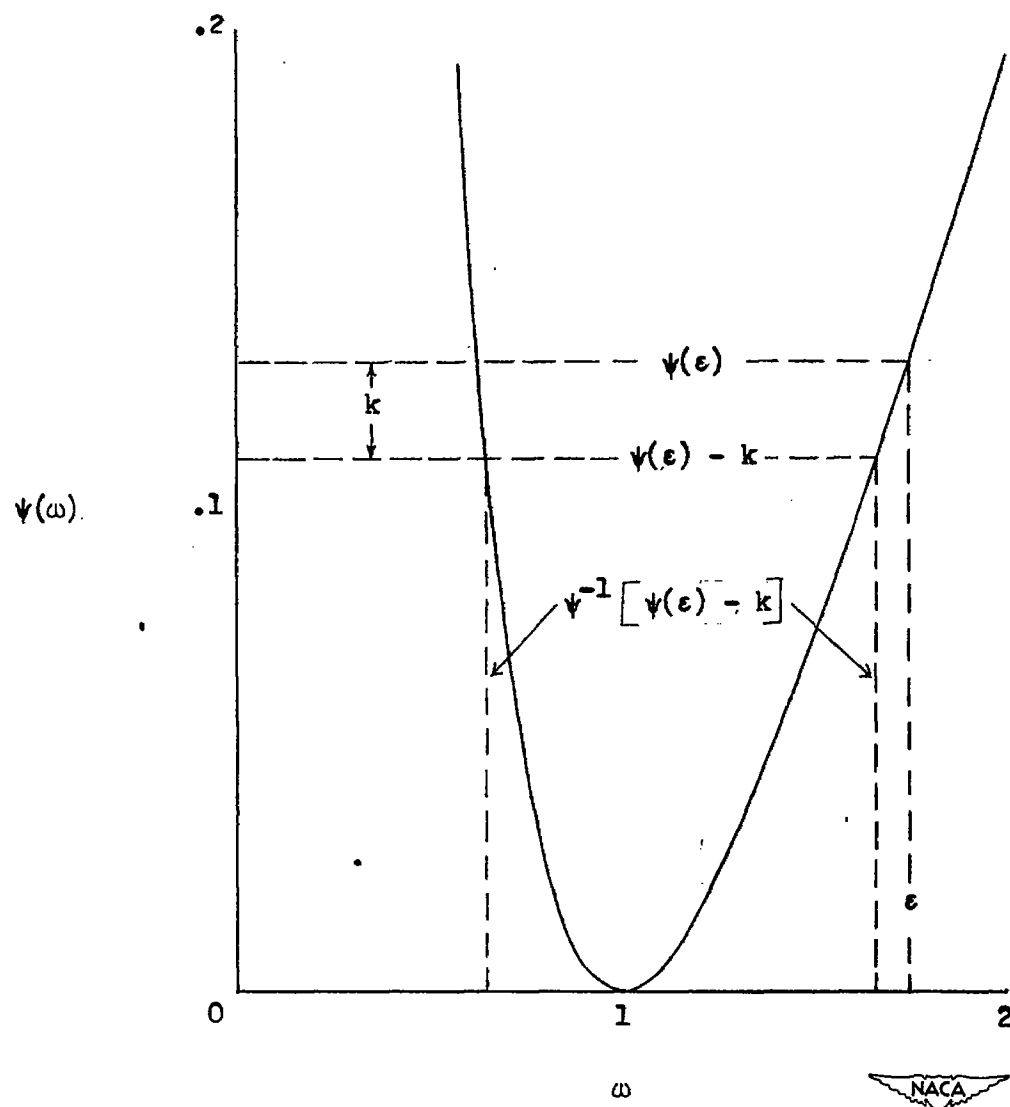


Figure 2.- Variation of the  $\psi$ -function.  $\psi(\omega) = \frac{1}{\omega} + \log_e \omega - 1$ .



(b)  $0.8 < \omega < 1.2$ .

Figure 2.- Continued.



(c) Illustrative procedure for computing the inverse  $\psi$ -function.

Figure 2.- Concluded.

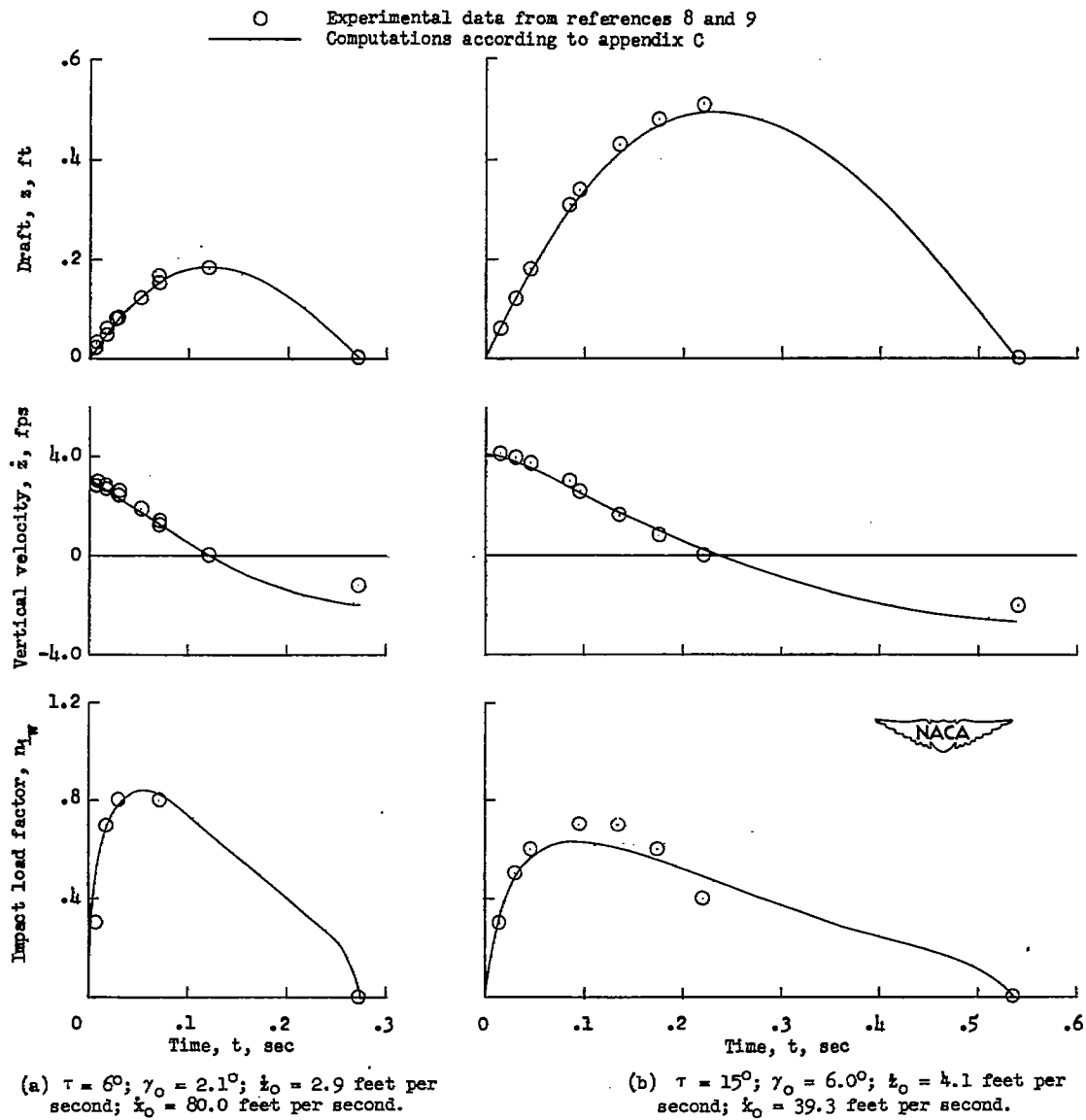


Figure 3.- Comparison of calculated and experimental loads and motions for a rectangular flat plate with a beam-loading coefficient of 18.8.

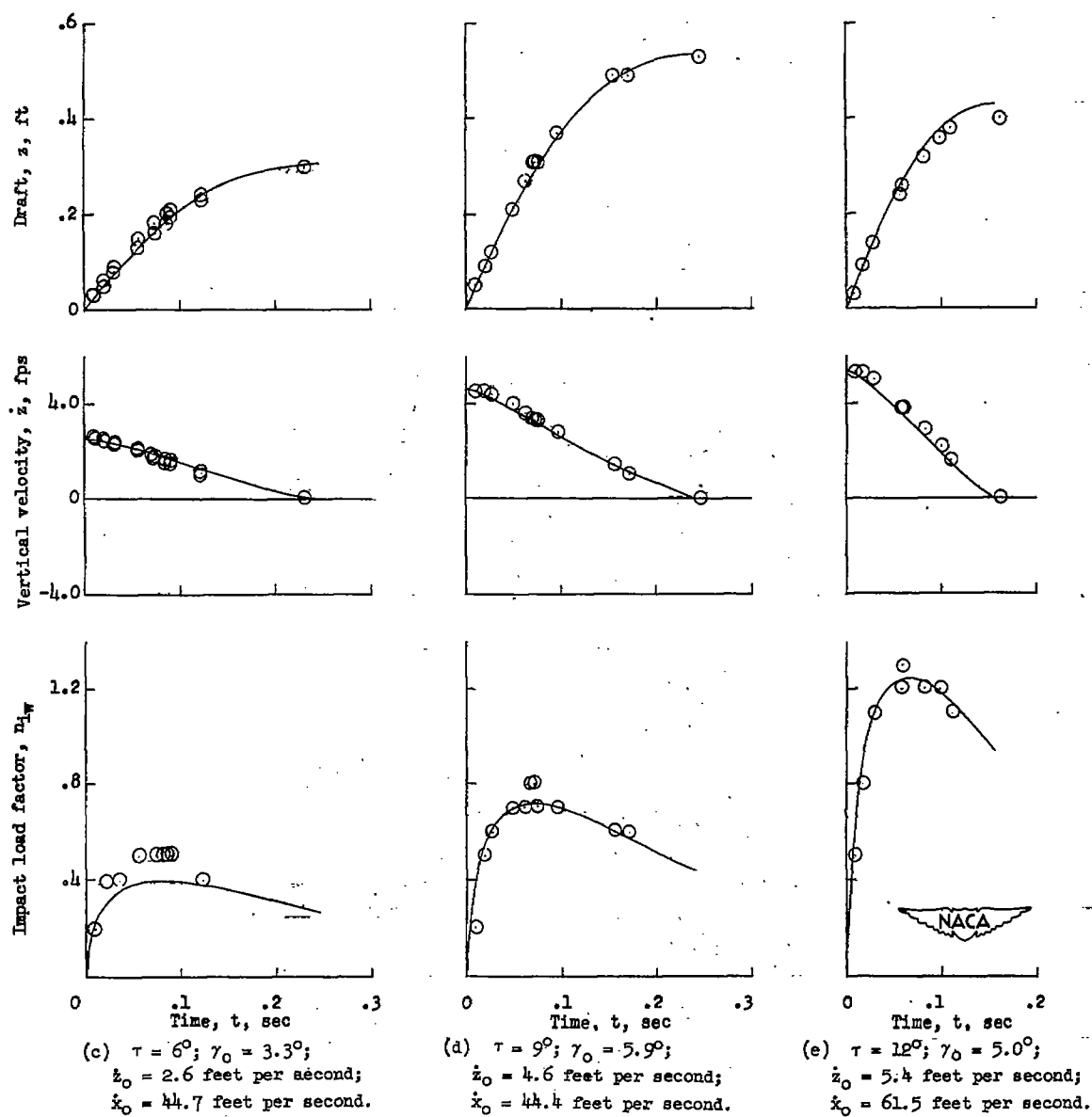
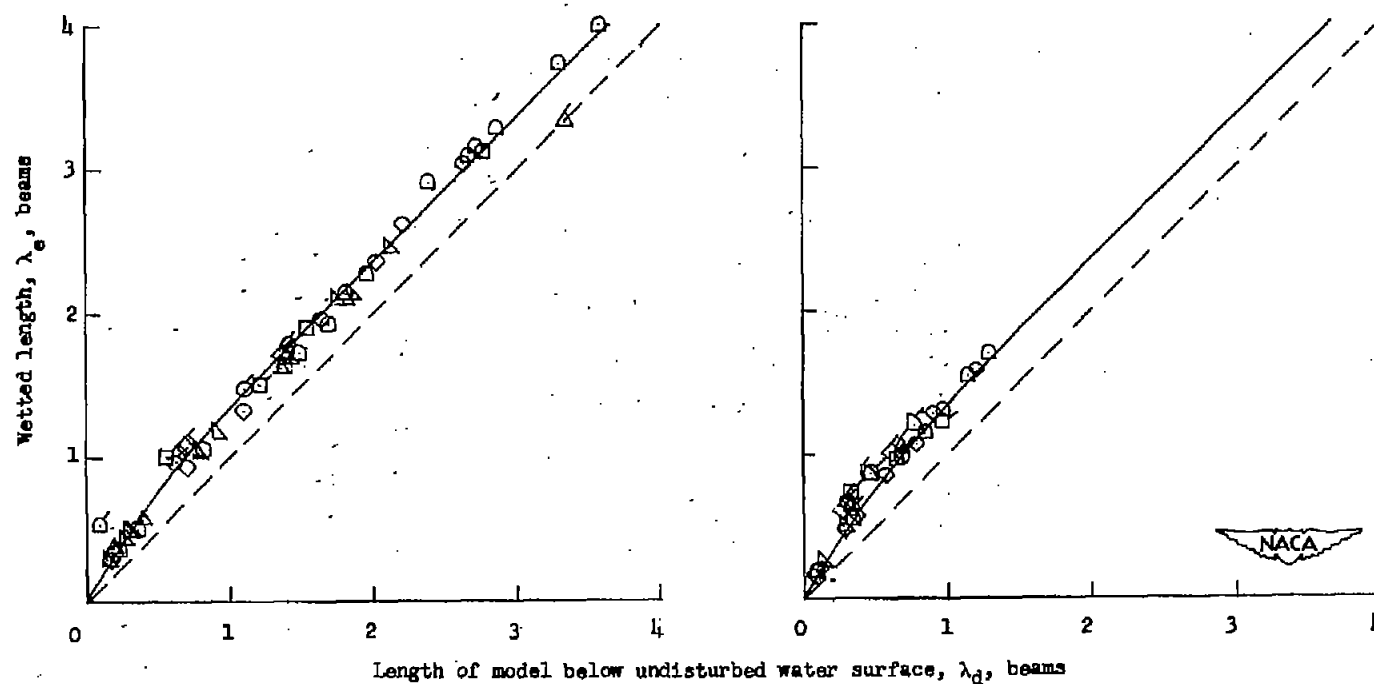


Figure 3.- Concluded.

$\text{--- Empirical equation } \begin{cases} \lambda_e = 1.7\lambda_d - 0.35\lambda_d^2 & \text{when } \lambda_d < 1 \\ \lambda_e = \lambda_d + 0.35 & \text{when } \lambda_d > 1 \end{cases}$   
 $\text{--- } \lambda_e = \lambda_d$

$C_V$	13.1	9.3	6.9	5.5	4.7	4.3	3.5	2.3
Reference 10				$\Delta$	$\Delta$		$\square$	$\diamond$
Reference 12	$\circ$	$\square$	$\diamond$	$\Delta$		$\nabla$	$\square$	

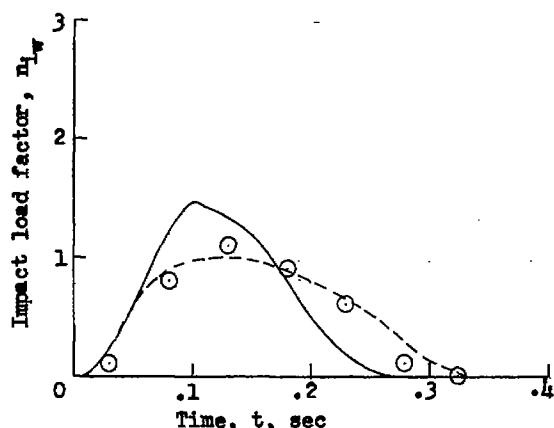


(a)  $5^\circ < \tau < 7^\circ$ .

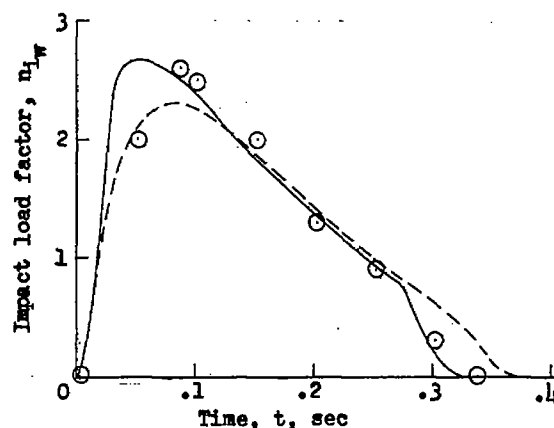
(b)  $9^\circ < \tau < 18^\circ$ .

Figure 4.- The increase in wetted length due to wave rise for a rectangular flat plate during steady planing.  $\lambda_d = \frac{z}{b \sin \tau}$ .

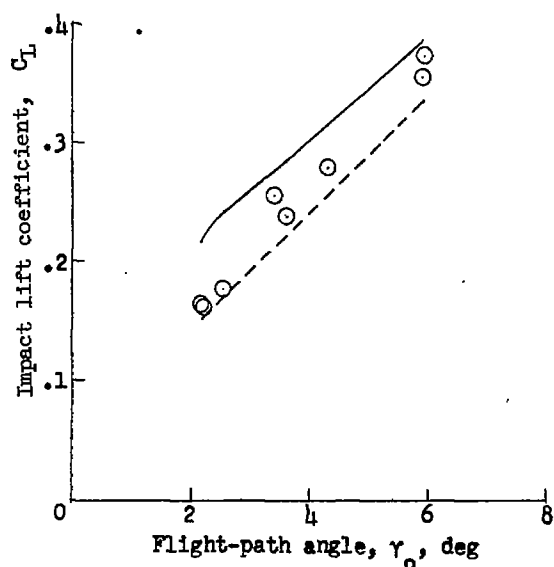
- Experimental data obtained from tests described in reference 23  
 — Impact computations based on analysis of reference 6  
 - - - Impact computations based on analysis of reference 15



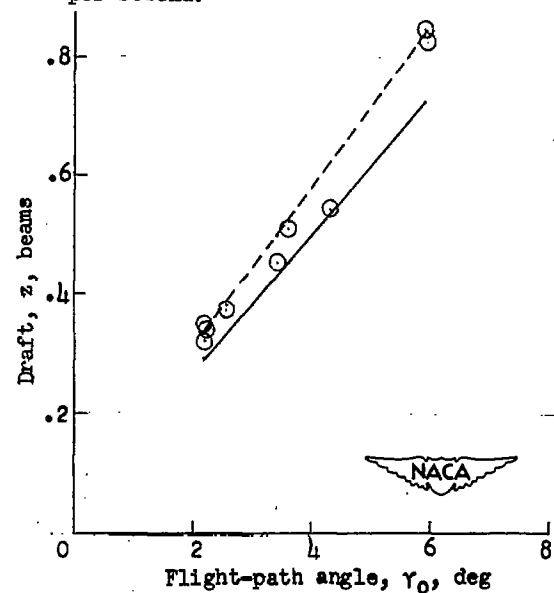
(a) Impact load time history.  $\gamma_0 = 2.2^\circ$ ;  $\dot{z}_0 = 3.4$  feet per second;  $\dot{x}_0 = 89.3$  feet per second.



(b) Impact load time history.  $\gamma_0 = 5.9^\circ$ ;  $\dot{z}_0 = 9.4$  feet per second;  $\dot{x}_0 = 90.9$  feet per second.



(c) Maximum loads.

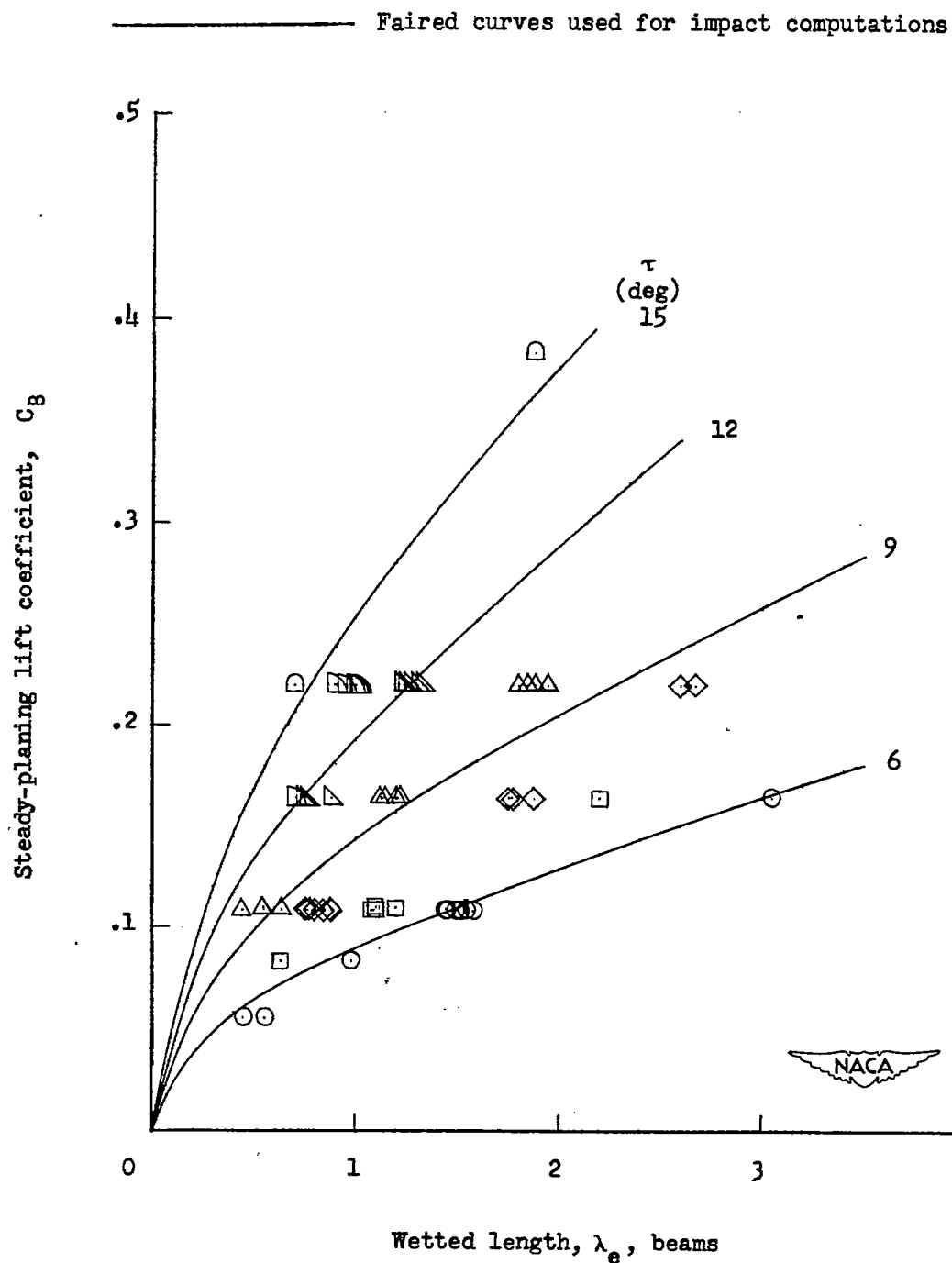


(d) Maximum drafts.

Figure 5.- Comparison of calculated and experimental loads and drafts for a prismatic model with an angle of dead rise of  $30^\circ$ , a beam-loading coefficient of 18.8, and a trim of  $15^\circ$ .

	○	□	◇	△	▴	▾	◻
$\tau$ , deg	6	7	8	10	12	14	16

Experimental data from reference 7

Figure 6.- High-speed steady-planing data.  $\beta = 0^\circ$ .